

Surface Chemistry of C-N Bonds on Rh(111). 2. CH₃NO₂ and C₂H₅NO₂

S. Y. Hwang, A. C. F. Kong, and L. D. Schmidt*

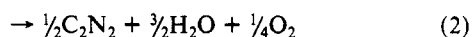
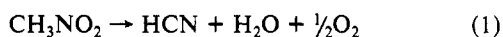
Department of Chemical Engineering and Materials Science, University of Minnesota, Minneapolis, Minnesota 55455. (Received: January 23, 1989; In Final Form: June 27, 1989)

The adsorption and decomposition of CH₃NO₂ and C₂H₅NO₂ on Rh(111) and C₂H₅NO₂ on Pt(111) have been studied by using temperature-programmed desorption (TPD) and Auger electron spectroscopy (AES). TPD following adsorption of CH₃NO₂ on Rh(111) produces complete decomposition with CO, N₂, H₂, and CO₂ as major products, smaller amounts of CH₄, and trace amounts of HCN, NO, and H₂O. The major decomposition path of CH₃NO₂ adsorbed on Rh(111) is therefore complete dissociation of the C-N and N-O bonds leaving adsorbed N and O atoms and surface CH_x species which dehydrogenate between 500 and 640 K. This is in sharp contrast with Pt(111) on which no C-N bonds are broken and C₂N₂ is the primary product. TPD of C₂H₅NO₂ on Rh(111) at 300 K also produces complete decomposition with C₂H₄ 70% of C₂H₅NO₂ at saturation, O₂, and N₂ as major products, smaller amounts of CO and CO₂, and trace amounts of H₂O and NO. The C₂H₄ desorbs at ~620 K, which suggests that some adsorbed species with C-C and C-H bonds intact must be stable to this temperature. The desorption of O₂ at high temperatures suggests that some of the oxygen is bound in some form which is unable to react with C or H until all of these species desorb. Thermal desorption of C₂H₅NO₂ on Pt(111) at 300 K produces NO and H₂ as major products, smaller amounts of CO and C₂N₂, and traces of C₂H₄, CO₂, and H₂O. The H₂ desorption spectra from C₂H₅NO₂ adsorption match those from C₂H₄ adsorption on Pt(111). The major decomposition path of C₂H₅NO₂ on Pt(111) is scission of the C-N bonds producing NO and leaving hydrocarbon fragments such as ethylidyne (≡C-CH₃) which dehydrogenate between 500 and 720 K to leave surface carbon residues. The stabilities of the C-N bond in C₂H₅NO₂ on Rh(111) and Pt(111) are therefore quite different in that 40% of the C-N bond is preserved on Pt(111) while it is completely cleaved on Rh(111).

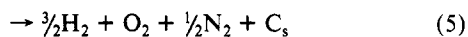
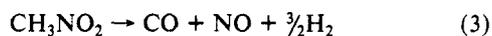
Introduction

Recently we investigated the adsorption and decomposition of CH₃NO₂¹ and CH₃NH₂² on Pt(111) with TPD, AES, and X-ray photoelectron spectroscopy (XPS). We found that C-N bonds in these molecules are very stable on Pt(111) in that no significant C-N bond scission is observed in TPD up to 1250 K. In this study, we use TPD and AES to examine the adsorption and decomposition of CH₃NO₂ and C₂H₅NO₂ on Rh(111).

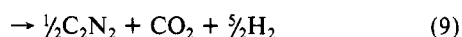
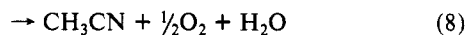
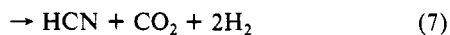
Nitromethane decomposition can occur by C-H and N-O bond scission



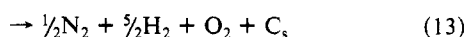
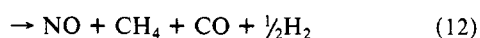
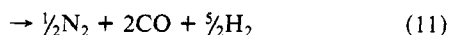
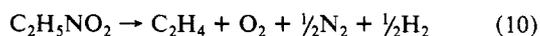
or through C-N bond breaking:



Nitroethane decomposition on metal surfaces has more decomposition products but basically can occur by scission of C-H, N-O, and C-C bonds



or by C-N bond breaking:



Except with CH₃CN and C₂H₄ formation, one expects surface

carbon residues from most reactions unless carbon oxidation is sufficiently efficient.

CH₃NO₂ decomposition has been studied on Pt(111) by TPD, AES, and XPS¹ and on Ni(111) by AES, TPD, and IR spectroscopy.³ On Ni(111), nitromethane decomposed by scission of the N-O bonds forming primarily HCN (34%), H₂ (41%), and CO (12%), leaving ~65% of the oxygen atoms adsorbed on the surface after the crystal was annealed to 1000 K.³ Small amounts of N₂ (2%), NH₃ (5%), H₂O (2%), and CO₂ (2%) were also detected. The saturation coverage at 300 K was estimated to be ~0.3 monolayer or 5.6 × 10¹⁴ molecules/cm².

On Pt(111), nitromethane decomposes by scission of C-H bonds (which form H₂ and H₂O) and N-O bonds (which form H₂O, CO, and NO) to leave adsorbed CN which desorbs as the dimer C₂N₂ (>85%) between 750 and 1200 K.¹ TPD and XPS experiments suggest that CH₃NO₂ decomposes to a certain surface intermediate CH_xNO_y by 300 K, followed by complete deoxygenation to CH_xN by ~500 K, then complete dehydrogenation to CN by ~750 K, which then desorbs as C₂N₂ between 750 and 1200 K. CH₃NO₂ saturation coverage was estimated to be (2.2 ± 0.4) × 10¹⁴ molecules/cm² by calibrations of TPD peak areas, AES N (379 eV) peak height, and XPS N(1s) peak area. Adsorption of CH₃NO₂ produces a CH₃NO₂ second monolayer peak at 165 K and a CH₃NO₂ multilayer layer at 141 K.

Experimental Section

Experiments were performed in a stainless steel vacuum system with a base pressure of 3 × 10⁻¹⁰ Torr. The procedures used for crystal preparation, cleaning, and TPD were described in the companion paper on C₂N₂ and CH₃NH₂ and in our previous work.¹ Yields of various desorption products from TPD experiments on Rh(111) were calibrated against CO (assuming a CO saturation density of 1 × 10¹⁵ molecules/cm² on Rh(111) at 300 K⁴), NO (1.1 × 10¹⁵ molecules/cm² on Rh(111) at 100 K⁵), H₂ (8 × 10¹⁴ molecules/cm² on Rh(111) at 100 K⁶), and O₂ (6.5 × 10¹⁴ molecules/cm² on Rh(111) at 300 K⁵). Yields from the thermal desorption of C₂H₅NO₂ on Pt(111) were calibrated against C₂N₂ (3 × 10¹⁴ molecules/cm² on Pt(111) at 300 K^{1,7}),

(3) Benziger, J. B. *Appl. Surf. Sci.* **1984**, *17*, 309.

(4) Castner, D. G.; Sexton, B. A.; Somorjai, G. A. *Surf. Sci.* **1978**, *71*, 519.

(5) Root, T. W.; Schmidt, L. D.; Fisher, G. B. *Surf. Sci.* **1983**, *134*, 30.

(6) Yates, Jr., J. T.; Thiel, P. A.; Weinberg, W. H. *Surf. Sci.* **1979**, *84*, 427.

(7) Hoffmann, W.; Bertel, E.; Netzer, F. P. *J. Catal.* **1979**, *60*, 316.

(1) Hwang, S. Y.; Kong, A. C. F.; Schmidt, L. D. submitted for publication in *Surf. Sci.*

(2) Hwang, S. Y.; Seebauer, E. G.; Schmidt, L. D. *Surf. Sci.* **1987**, *188*, 219.

H₂ (6×10^{14} molecules/cm² on Pt(111) at 100 K⁸), CO (7×10^{14} molecules/cm² on Pt(111) at 300 K^{9,10}), and NO (8×10^{14} molecules/cm² on Pt(111) at 100 K¹¹). The pumping speed and mass spectrometer sensitivity of other species were assumed to be the same as those of CO.

Nitromethane (99+%, Aldrich) and nitroethane (99.5+%, Aldrich), both liquid at room temperature with vapor pressures of ~ 40 Torr, were degassed and further purified by several freeze-pump cycles until no impurities were evident in the mass spectrum. NO (99%), CO (99.99%), C₂H₄ (99.99%), and H₂ (99.9995%) were used for cleaning and calibration of TPD yield without further purification. CH₃CN (99.9+%, Aldrich) was degassed and further purified by freeze-pump cycles before its cracking pattern was determined. All gases were admitted into the vacuum system between 5×10^{-9} and 1×10^{-6} Torr.

In TPD survey spectra, Figures 1, 4, and 6, we examined all masses and the expected cracking fragments for reactants and products. Sensitivities and peak areas are not meant to be quantitative in these spectra, but all amounts are calculated in Table I.

Experiments were carried out for adsorption at 80 and 300 K. Below 300 K, condensation of less volatile species made it difficult to compare amounts desorbing quantitatively, and all spectra shown except for the parent species were obtained at 300 K. However, except for H₂ and H₂O, negligible desorption occurred below 300 K, so that spectra shown for 300 K adsorption represent those which would be observed for lower temperature adsorption except for the reactant molecules. Water was impossible to monitor quantitatively, and we were only able to estimate it by subtraction of H and O signals from other species.

A major assumption in interpreting TPD spectra is that TPD peaks probably arise from *decomposition-limited* processes if they occur significantly above the temperatures observed for those species alone. As examples, H₂, N₂, CH₄, H₂O, and CO₂ are all observed to desorb several hundred kelvin above temperatures where these gases alone would desorb. This interpretation is of course complicated by the coadsorption of other species. In general, we expect coadsorption to *lower* peak temperatures unless some type of attractive complex is formed. It should also be noted that variations in peaks with coverage include these interactions but that shifts to higher temperature with increasing coverage are an even stronger indication of decomposition-limited TPD.

Results

1. *CH₃NO₂ on Rh(111)*. Thermal desorption of CH₃NO₂ adsorbed on Rh(111) at 300 K produces CO, N₂, CO₂, and H₂ as major products as summarized in Figure 1 for a 10-langmuir exposure. Smaller amounts of CH₄, HCN, H₂O, and NO were also detected. The *m/e* = 17 spectrum shows only peaks characteristic of the cracking pattern of H₂O and no production of NH₃. No desorption of CH₃NO₂, C₂N₂, NO₂, or O₂ was detected. TPD experiments with the crystal ramped to 1400 K revealed no desorption of oxygen, which is known to desorb above 1000 K at low coverages on Rh(111),^{4,12,13} although O₂ was observed from C₂H₅NO₂ as will be described later. In fact, no species were detected desorbing between 1000 and 1400 K.

Figure 2 shows TPD spectra of (a) H₂, (b) CO + N₂ (*m/e* = 28), (c) N₂ (*m/e* = 14), and (d) CO₂ from indicated CH₃NO₂ exposures on Rh(111) at 300 K. Hydrogen desorption from CH₃NO₂ TPD exhibits at least three desorption peaks at 370, 480, and 630 K. The 370 K peak, as the 370 K hydrogen peak in CH₃NH₂ TPD experiments in the companion paper, may arise from partial dehydrogenation of the first few CH₃NO₂ molecules upon adsorption on Rh(111) at 300 K. This peak, however, does not grow or shrink significantly with increasing CH₃NO₂ exposure

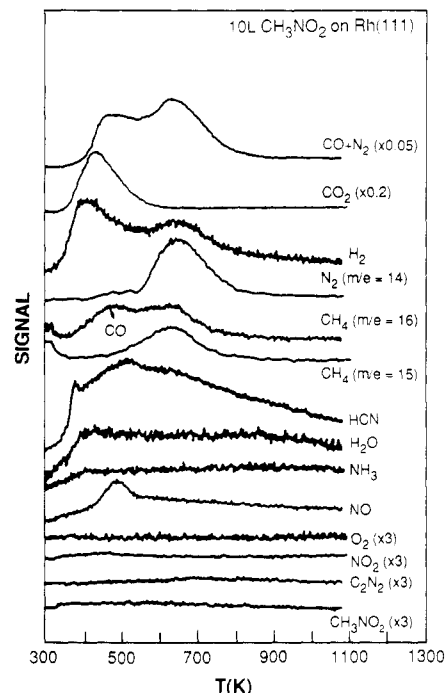


Figure 1. TPD spectra of CH₃NO₂ and its reaction products on Rh(111) following 10 langmuirs of CH₃NO₂ exposure at 300 K. The heating rate β was ~ 22 K/s at 300 K and ~ 16 K/s at 1000 K.

as in CH₃NH₂ experiments. No significant shift in peak temperature was observed for the three higher temperature peaks and only the 630 K peak shows significant growth with increasing CH₃NO₂ exposure. Hydrogen TPD spectra saturate at ~ 40 langmuirs.

At very low coverages (< 0.5 langmuir), TPD spectra at 28 amu (CO + N₂) exhibits at least three peaks at 510, 580, and 710 K (Figure 2b). All of the three peaks grow and shift to lower temperature with increasing CH₃NO₂ exposure until they saturate at ~ 10 langmuirs. The two peaks at 510 and 580 K are from CO desorption since they also appear in 16 amu (Figure 1) and 12 amu spectra (not shown). Since CO adsorbed on Rh(111) at 300 K desorbs at ~ 500 K at low coverages and shifts to lower temperature with increasing exposure,^{12,14,15} the 510 K peak is desorption limited, while the 580 K peak is reaction limited. The two peaks shift to 480 and 560 K at 10 langmuirs.

The 28 amu peak at 710 K is attributed to nitrogen because it also appears in the 14 amu spectra (Figure 2c) but not in the 12 or 16 amu spectra. This peak is more than 100 K lower in peak temperature than the nitrogen peak from C₂N₂ and CH₃NH₂ exposures, indicating a different desorption process; it also shifts to lower temperature with increasing coverage rather than upward as with C₂N₂ and CH₃NH₂. At 10 langmuirs, the peak shifts to ~ 660 K, which is comparable to the nitrogen desorption temperature from NO^{15,16} and HNCO¹⁷ exposures on Rh(111). Since HNCO decomposes completely by 390 K on Rh(111) to give adsorbed CO and N atoms which recombine and desorb as N₂ at ~ 670 K,¹⁷ it is very likely that nitrogen desorption from CH₃NO₂ exposure arises from a similar process: recombination of N atoms from partial decomposition of CH₃NO₂ at lower temperature. The shift to lower temperature of the N₂ desorption peak, as expected for second-order desorption kinetics, also supports this mechanism.

CO₂ desorption from CH₃NO₂ exposure (Figure 2d) exhibits two peaks at 490 and 560 K at 1 langmuir. Both peaks grow continuously and shift to lower temperature with increasing coverage until they saturate at ~ 20 langmuirs with peak tem-

(8) Christmann, K.; Ertl, G.; Pignet, T. *Surf. Sci.* **1976**, *54*, 365.

(9) Ogletree, D. F.; Van Hove, M. A.; Somorjai, G. A. *Surf. Sci.* **1986**, *173*, 351.

(10) Ertl, G.; Neumann, M.; Streit, K. M. *Surf. Sci.* **1977**, *64*, 393.

(11) Gorte, R. J.; Schmidt, L. D.; Gland, J. L. *Surf. Sci.* **1981**, *109*, 367.

(12) Hwang, S. Y. Ph.D. Thesis, University of Minnesota, 1988, to be published.

(13) Wagner, F. T.; Moylan, T. E. *Surf. Sci.* **1987**, *191*, 121.

(14) Thiel, P. A.; Williams, E. D.; Yates, Jr., J. T.; Weinberg, W. H. *Surf. Sci.* **1979**, *84*, 54.

(15) Root, T. W.; Schmidt, L. D.; Fisher, G. B. *Surf. Sci.* **1985**, *150*, 173.

(16) Bugyi, L.; Solymosi, F. *Surf. Sci.* **1987**, *188*, 475.

(17) Kiss, J.; Solymosi, F. *Surf. Sci.* **1983**, *135*, 243.

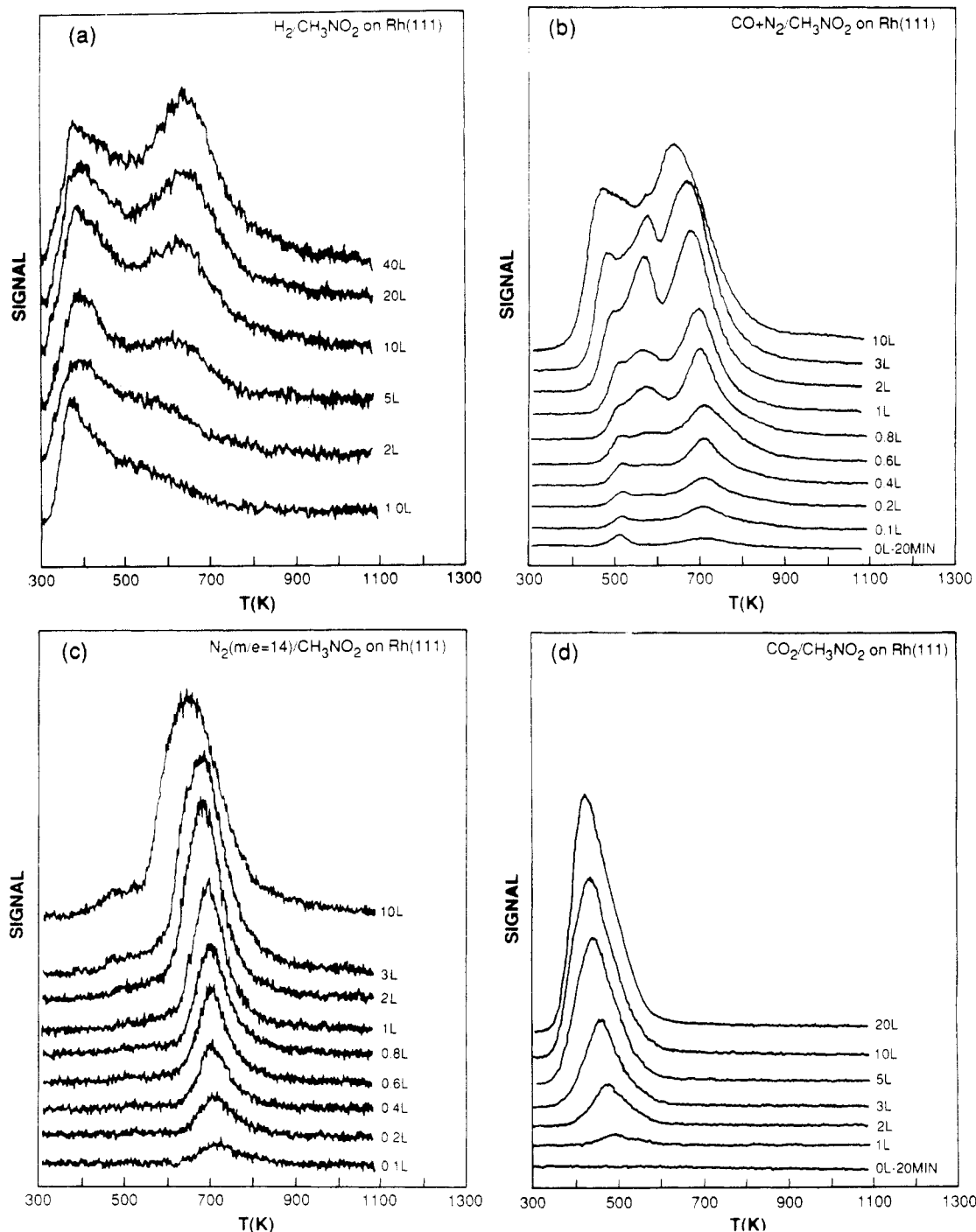


Figure 2. TPD spectra of (a) H_2 , (b) $\text{CO} + \text{N}_2$, (c) N_2 ($m/e = 14$), and (d) CO_2 on $\text{Rh}(111)$ following indicated CH_3NO_2 exposures at 300 K. The heating rate β was ~ 22 K/s at 300 K and ~ 16 K/s at 1000 K.

peratures of 405 and 480 K. The peak at 405 K is comparable to the CO_2 desorption temperature in $\text{CO} + \text{NO}$ TPD on $\text{Rh}(111)$ ¹⁵ and in thermal desorption of HNCO on an oxygen-predeposited $\text{Rh}(111)$ surface.¹⁸ Both desorption peaks of CO_2 should be reaction limited since CO_2 adsorbs only weakly on $\text{Rh}(111)$ at 120 K and desorbs by 350 K.¹⁵ Root et al.¹⁵ observed that CO_2 from TPD of both $\text{CO} + \text{NO}$ and $\text{CO} + \text{O}_2$ desorbs as peaks at ~ 425 K (shifts to lower temperature) with a leading edge that begins at ~ 350 K. The similarity between these observations and the CH_3NO_2 desorption spectra (Figure 2d) suggest that the CO_2 desorption peak at 405 K from CH_3NO_2 exposures may arise from the $\text{CO}_{\text{ad}} + \text{O}_{\text{ad}} \rightarrow \text{CO}_2$ reaction, which is suggested to be the common rate-limiting step in both $\text{CO} + \text{NO}$ and $\text{CO} + \text{O}_2$ experiments.¹⁵

At low coverages, methane desorbs from CH_3NO_2 exposures (data not shown) as a single symmetric peak at 595 K. This peak shifts to higher temperature and grows with increasing CH_3NO_2 exposure until it saturates at ~ 40 langmuirs. HCN desorption (data not shown) shows only a broad background at low coverages (< 5 langmuirs). Above 5 langmuirs, at least two small peaks appear at 380 and 510 K. Both peaks saturate at ~ 20 langmuirs. As noted previously, H_2O was impossible to determine quantitatively because of desorption near 300 K and because no sharp peaks were observed.

Adsorption of CH_3NO_2 at 100 K (Figure 3) produces a CH_3NO_2 second monolayer peak at ~ 200 K and a CH_3NO_2 multilayer peak at ~ 165 K. The second monolayer peak shifts to lower temperatures with increasing exposure and saturates at ~ 12 langmuirs with a peak temperature of ~ 180 K, while the multilayer peak at 165 K continues to grow beyond 30 langmuirs.

(18) Solymosi, F.; Berkó, A.; Tarnóczy, T. I. *Appl. Surf. Sci.* **1984**, *18*, 233.

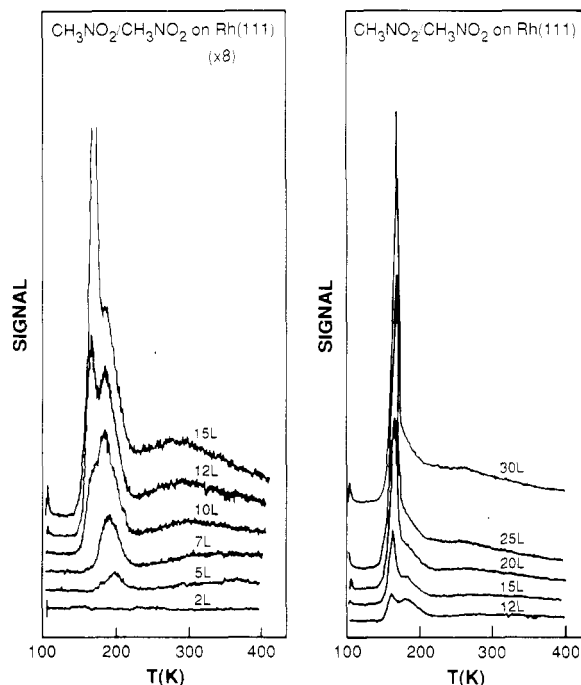


Figure 3. TPD spectra of CH_3NO_2 ($m/e = 61$) on Rh(111) following indicated CH_3NO_2 exposures at 100 K. The second monolayer peak at 200 K saturates at ~ 12 langmuirs while the multilayer ice peak at 165 K continues to grow beyond 30 langmuirs. The heating rate β was ~ 10 K/s up to 400 K.

2. $\text{C}_2\text{H}_5\text{NO}_2$ on Rh(111). Thermal desorption of 10 langmuirs of $\text{C}_2\text{H}_5\text{NO}_2$ adsorbed on Rh(111) at 300 K (Figure 4) produces O_2 , CO , N_2 , H_2 , CO_2 , and C_2H_4 as major products, smaller amounts of H_2O and NO , and traces of HCN and CH_4 . The 17 amu spectrum shows only the cracking pattern of H_2O , indicating that no NH_3 desorbs. No desorption of NO_2 , C_2N_2 , CH_3NO_2 , CH_3CN , or $\text{C}_2\text{H}_5\text{NO}_2$ was detected.

Figure 5 shows TPD of (a) O_2 , (b) H_2 , (c) 28 amu ($\text{CO} + \text{N}_2 + \text{C}_2\text{H}_4$), (d) CO ($m/e = 16$), (e) C_2H_4 ($m/e = 26$), and (f) CO_2 from indicated $\text{C}_2\text{H}_5\text{NO}_2$ exposures on Rh(111) at 300 K. No oxygen desorption (Figure 5a) was observed at low $\text{C}_2\text{H}_5\text{NO}_2$ coverages (< 5 langmuirs). At 5 langmuirs, oxygen desorbs as a symmetric peak at 1235 K. The peak shifts downward with increasing coverage and saturates below 50 langmuirs with a peak temperature of ~ 1190 K, which is comparable to the oxygen desorption temperature (1200 K) from NO decomposition and from oxygen adsorption (at low coverage) on Rh(111).⁵

Hydrogen desorption from $\text{C}_2\text{H}_5\text{NO}_2$ (Figure 5b) is similar to that from CH_3NO_2 in that H_2 desorbs from both adsorbates as several overlapping peaks to form a continuous band from 300 to ~ 750 K. Hydrogen desorbs at least as five overlapping peaks at 370, 420, 460, 560, and 620 K. At low coverages (< 2 langmuirs), however, the 370 K peak is well-defined and is the only major peak. This peak may arise from dehydrogenation of the first few $\text{C}_2\text{H}_5\text{NO}_2$ molecules upon adsorption on Rh(111) at 300 K, as the same H_2 peak observed in the thermal desorption of CH_3NH_2 and CH_3NO_2 . As with CH_3NH_2 , this peak is significantly reduced with increasing $\text{C}_2\text{H}_5\text{NO}_2$ exposure, possibly due to blocking of adsorbed H atoms by more $\text{C}_2\text{H}_5\text{NO}_2$ molecules adsorbed on the surface.

The 420 K peak is barely detectable as a shoulder of the 370 K peak at 0.5 langmuir, but it continues to grow with increasing $\text{C}_2\text{H}_5\text{NO}_2$ exposure, while the 370 K peak continues to shrink. At 2 langmuirs, this peak becomes comparable to the 370 K peak and becomes dominant over the 370 K peak above 5 langmuirs. Although the characterization of these two peaks is difficult due to strong overlapping, the 2 langmuir spectrum clearly indicates two distinct peaks. The two highest temperature peaks at 560 and 620 K emerge at ~ 5 langmuirs and continue to grow and saturate at ~ 100 langmuirs. The peak at 460 K becomes detectable at ~ 10 langmuirs. It grows and shifts upward with

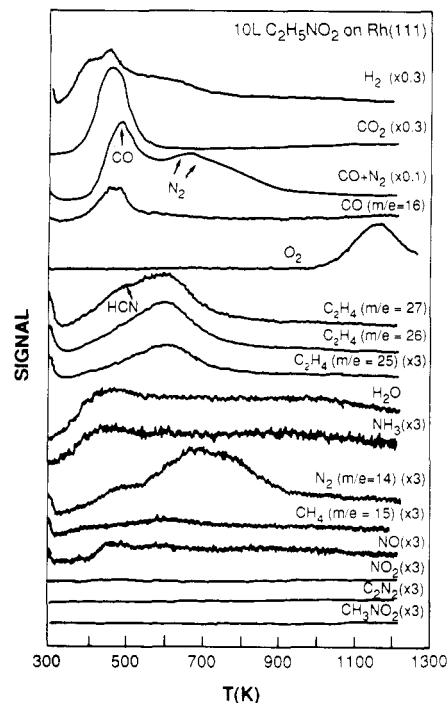


Figure 4. TPD spectra of the reaction products of $\text{C}_2\text{H}_5\text{NO}_2$ on Rh(111) following 10 langmuirs of $\text{C}_2\text{H}_5\text{NO}_2$ exposure at 300 K. The heating rate β was ~ 34 K/s at 300 K and ~ 26 K/s at 1000 K.

increasing $\text{C}_2\text{H}_5\text{NO}_2$ coverage until it saturates at ~ 100 langmuirs.

Comparison of the hydrogen desorption spectra from $\text{C}_2\text{H}_5\text{NO}_2$ adsorption on Rh(111) to those from C_2H_4 on Rh(111)¹⁹ reveals great similarities between the two adsorbates. On Rh(111), adsorption of C_2H_4 at low temperatures produces a stable ethylidyne ($\equiv\text{C}-\text{CH}_3$) species at 310 K²⁰ which dehydrogenates between 360 and 750 K with a single hydrogen desorption peak at 440 K followed by continuous H_2 evolution until 750 K.¹⁹ A hydrogen desorption peak at 350 K was observed and attributed to chemisorbed hydrogen on the Rh(111) surface. The hydrogen desorption spectra from $\text{C}_2\text{H}_5\text{NO}_2$ and C_2H_4 are therefore very similar in that both exhibit a chemisorbed hydrogen peak near 360 K, a major desorption peak near 450 K, and a continuous H_2 evolution band up to 750 K. This suggests that the hydrogen desorption from $\text{C}_2\text{H}_5\text{NO}_2$ adsorption on Rh(111) may arise from the dehydrogenation of certain C_2H_x species, most likely ethylidyne as from C_2H_4 adsorption.

The 28 amu TPD spectra (Figure 5c) involve signals from at least three molecules: CO , C_2H_4 , and N_2 . The 16 amu (Figure 5d) and 12 amu (data not shown) spectra suggest that the peak at ~ 500 K arises from desorption of CO . This peak starts at ~ 515 K, grows, and shifts to lower temperature with increasing $\text{C}_2\text{H}_5\text{NO}_2$ coverage and saturates at ~ 100 langmuirs. The small shoulder at ~ 600 K in the 16 amu spectra (Figure 5d), detectable only above 10 langmuirs, is attributed to a cracking fragment of C_2H_4 in mass spectrometer.

The nitrogen desorption (Figure 5c) spectrum at 0.5 langmuir shows a least two peaks at 750 and 810 K. Both peaks shift downward with increasing $\text{C}_2\text{H}_5\text{NO}_2$ exposure until they saturate at ~ 10 langmuirs with peak temperatures of 680 and 760 K. The peak at 680 K coincides with the N_2 desorption peak from HNCO and CH_3NO_2 . It is therefore attributed to recombination of N atoms arising from scission of C-N and N-O bonds at lower temperature, as in CH_3NO_2 .

The 27, 26, 25 (Figure 4), and 24 amu (data not shown) TPD spectra at 10 langmuirs all show a peak at ~ 600 K, suggesting that the peak should arise from desorption of C_2H_4 . The ratio

(19) Dubois, L. H.; Castner, D. G.; Somorjai, G. A. *J. Chem. Phys.* **1980**, *72*, 5234.

(20) Koel, B. E.; Bent, B. E.; Somorjai, G. A. *Surf. Sci.* **1984**, *146*, 211.

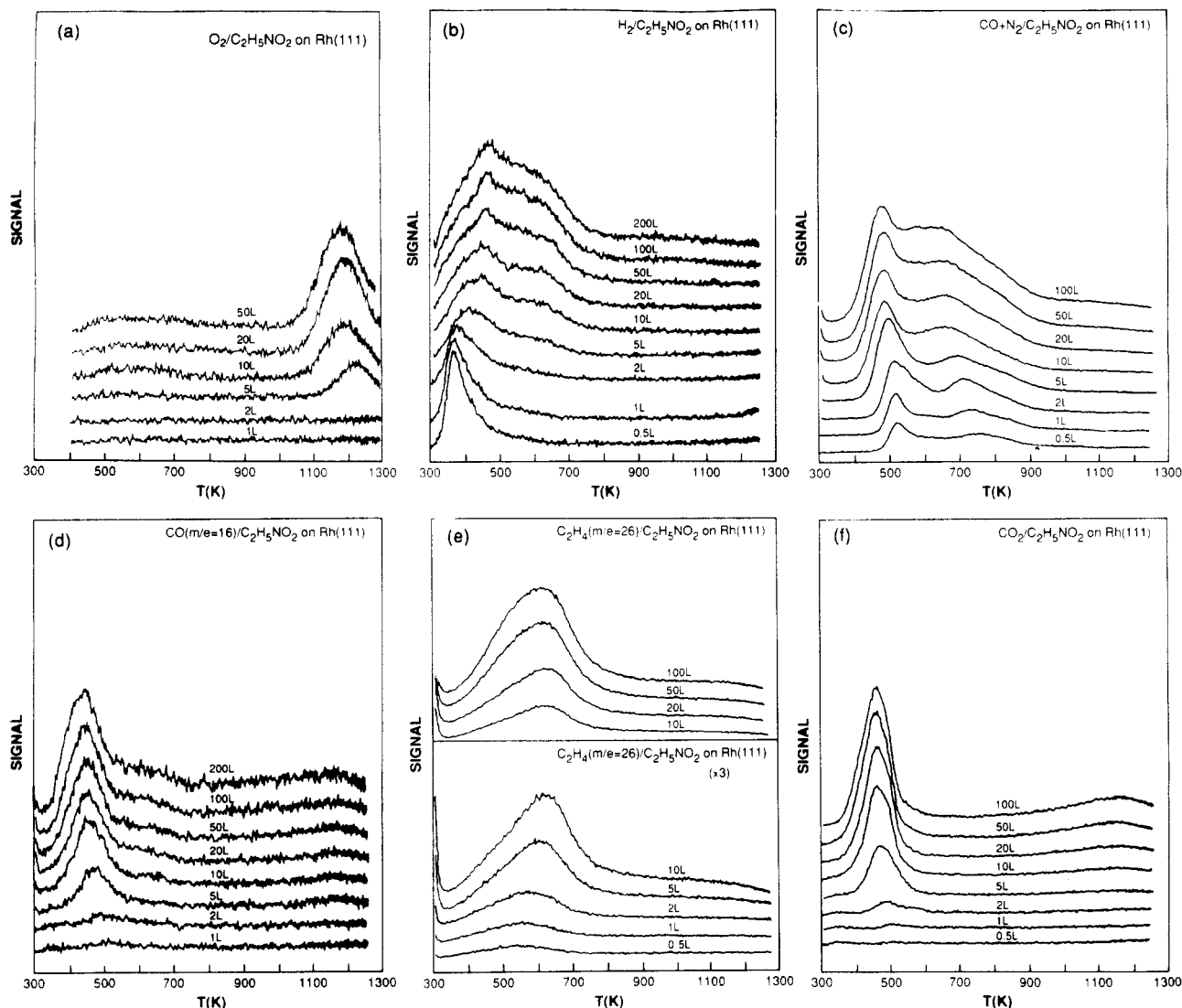


Figure 5. TPD spectra of (a) O_2 , (b) H_2 , (c) $CO + C_2H_4 + N_2$, (d) CO ($m/e = 16$), (e) C_2H_4 ($m/e = 26$), and (f) CO_2 on $Rh(111)$ following $C_2H_5NO_2$ exposures indicated at 300 K. The heating rate β was ~ 34 K/s at 300 K and ~ 26 K/s at 1000 K.

of the peak heights of these spectra is within 4% of the cracking pattern of C_2H_4 in the mass spectrometer. The cracking pattern of C_2H_4 in the mass spectrometer indicates that the 28 amu TPD spectra (Figures 4 and 5c) should show a peak $\sim 84\%$ bigger than the 27 amu peak at ~ 600 K. Such a peak is not observed because it is buried under the huge 28 amu desorption band between 400 and 900 K.

The C_2H_4 peak (Figure 5e) starts at ~ 550 K at 0.5 langmuir, grows and shifts to higher temperature with increasing $C_2H_5NO_2$ coverage, and saturates at ~ 100 langmuirs with a peak temperature of 620 K. Spectra at $m/e = 25, 26$, and 27 show that there is no interference from HCN in analysis of C_2H_4 . Although C_2H_4 adsorbed on $Rh(111)$ at 300 K²¹ has been found to decompose to H_2 and surface carbon species upon heating, it was also found to desorb intact at 290 K on $Pt(111)$,^{22,23} at ~ 420 K on $Pt_{50}Ni_{50}(111)$,²⁴ at ~ 280 K on (1×1) $Pt(100)$,²⁵ at ~ 280 and 340 K on (5×20) $Pt(100)$,²⁵ and at ~ 270 K on $Ni(111)$.²⁶ It is also found to desorb as a self-hydrogenation product from adsorption of C_2H_2 on $Cu(110)$ at 340 K.²⁷

CO_2 desorption (Figure 5f) becomes detectable at ~ 2 langmuirs where one peak at ~ 490 K and a smaller peak at ~ 570 K are observed. Both peaks grow and shift downward with increasing $C_2H_5NO_2$ coverage until they saturate at ~ 100 langmuirs. At saturation, the two peaks are comparable in peak heights and have peak temperatures of ~ 430 and ~ 480 K. Both peaks are clearly reaction limited, like the CO_2 peak from CH_3NO_2 thermal desorption.

3. $C_2H_5NO_2$ on $Pt(111)$. Thermal desorption of 10 langmuirs of $C_2H_5NO_2$ adsorbed on $Pt(111)$ at 300 K (Figure 6) produces H_2 , NO , CO , and C_2N_2 as major products, smaller amounts of CO_2 and C_2H_4 , and traces of HCN and CH_4 . H_2O desorbs at ~ 450 K but its yield was not calibrated. The 17 amu spectrum in Figure 6 shows only the cracking pattern of H_2O , indicating that no NH_3 desorbs. No desorption of CH_3CN , NO_2 , N_2 , O_2 , CH_3NO_2 , or $C_2H_5NO_2$ was observed. Larger peaks near 300 K for masses of C_2H_4 on Pt obscure product analysis more than for Rh.

Figure 7 shows TPD spectra of (a) H_2 , (b) NO , (c) CO , (d) C_2N_2 , (e) CO_2 , and (f) C_2H_4 ($m/e = 26$) from $C_2H_5NO_2$ exposures indicated on $Pt(111)$ at 300 K. At low coverages (< 2 langmuirs), hydrogen desorbs as two major peaks at 410 and 530 K and a smaller peak at 440 K which is only detectable at 2 langmuirs. Since the desorption temperature of H_2 adsorbed on

(21) Castner, D. G.; Sexton, B. A.; Somorjai, G. A. *Surf. Sci.* **1978**, *71*, 519.

(22) Godbey, D.; Zaera, F.; Yeates, R.; Somorjai, G. A. *Surf. Sci.* **1986**, *167*, 150.

(23) Zhou, X.-L.; Zhu, X.-Y.; White, J. M. *Surf. Sci.* **1988**, *193*, 387.

(24) Abon, M.; Massardier, J.; Tardy, B.; Bertolini, J. C. *Surf. Sci.* **1987**, *189/190*, 880.

(25) Hatzikos, G. H.; Masel, R. I. *Surf. Sci.* **1987**, *185*, 479.

(26) Zaera, F.; Hall, R. B. *Surf. Sci.* **1987**, *180*, 1.

(27) Outka, D. A.; Friend, C. M.; Jorgensen, S.; Madix, R. J. *J. Am. Chem. Soc.* **1983**, *105*, 3468.

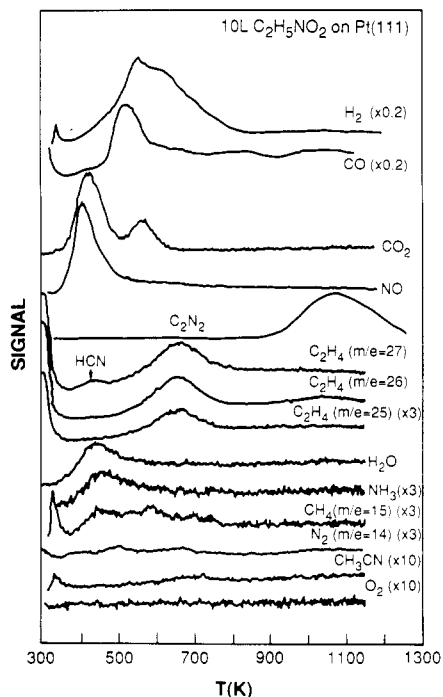


Figure 6. TPD spectra of the reaction products of $C_2H_5NO_2$ on Pt(111) following 10 langmuirs of $C_2H_5NO_2$ exposure at 300 K. The heating rate β was ~ 40 K/s at 300 K and ~ 30 K/s at 1000 K.

Pt(111) at 300 K is ~ 420 K,² the 410 K peak is desorption limited while the 530 K peak is reaction limited. With increasing $C_2H_5NO_2$ exposure, the two peaks at 440 and 530 K grow and shift up in temperature until they saturate at ~ 20 langmuirs with peak temperatures of 490 and 560 K. The peak at 420 K shrinks and shifts upward with increasing coverage and becomes a small shoulder of the 490 K peak at saturation. At least two additional peaks emerge at exposures above 5 langmuirs at ~ 640 and ~ 710 K. These two peaks do not shift with $C_2H_5NO_2$ exposure and are saturated at ~ 20 langmuirs.

Comparison of the hydrogen desorption spectra from $C_2H_5NO_2$ (Figure 7a) with those from C_2H_4 on Pt(111)^{23,28-30} indicates striking similarities between the thermal desorption of these two adsorbates on Pt(111). C_2H_4 adsorbed on Pt(111) at low temperatures (< 200 K) produces at least three hydrogen desorption peaks at 355, 450, and 530 K at low coverages.^{28,30} These three peaks shift up in temperature to 365, 495, and 550 K with increasing C_2H_4 coverage, while a new peak and shoulder at 645 and 710 K appear at higher C_2H_4 exposures.²⁸⁻³⁰ The peak at 495 K was attributed to dehydrogenation of the adsorbed ethylidyne species ($\equiv C-CH_3$) to some surface C_nH species ($n \leq 2$) and the peaks at 550, 645, and 710 K to complete dehydrogenation of this C_nH species to surface carbon residues.²⁹ The peak at 365 K matches that observed after low H_2 exposures^{8,30,31} and is not observed at high C_2H_4 exposures.^{29,30} It is therefore possibly due to background H_2 adsorption. This peak is not observed in this study, but instead, a desorption limited peak at 420 K is observed. The hydrogen desorption from $C_2H_5NO_2$ is therefore similar to that from C_2H_4 adsorption in that all the peaks observed from

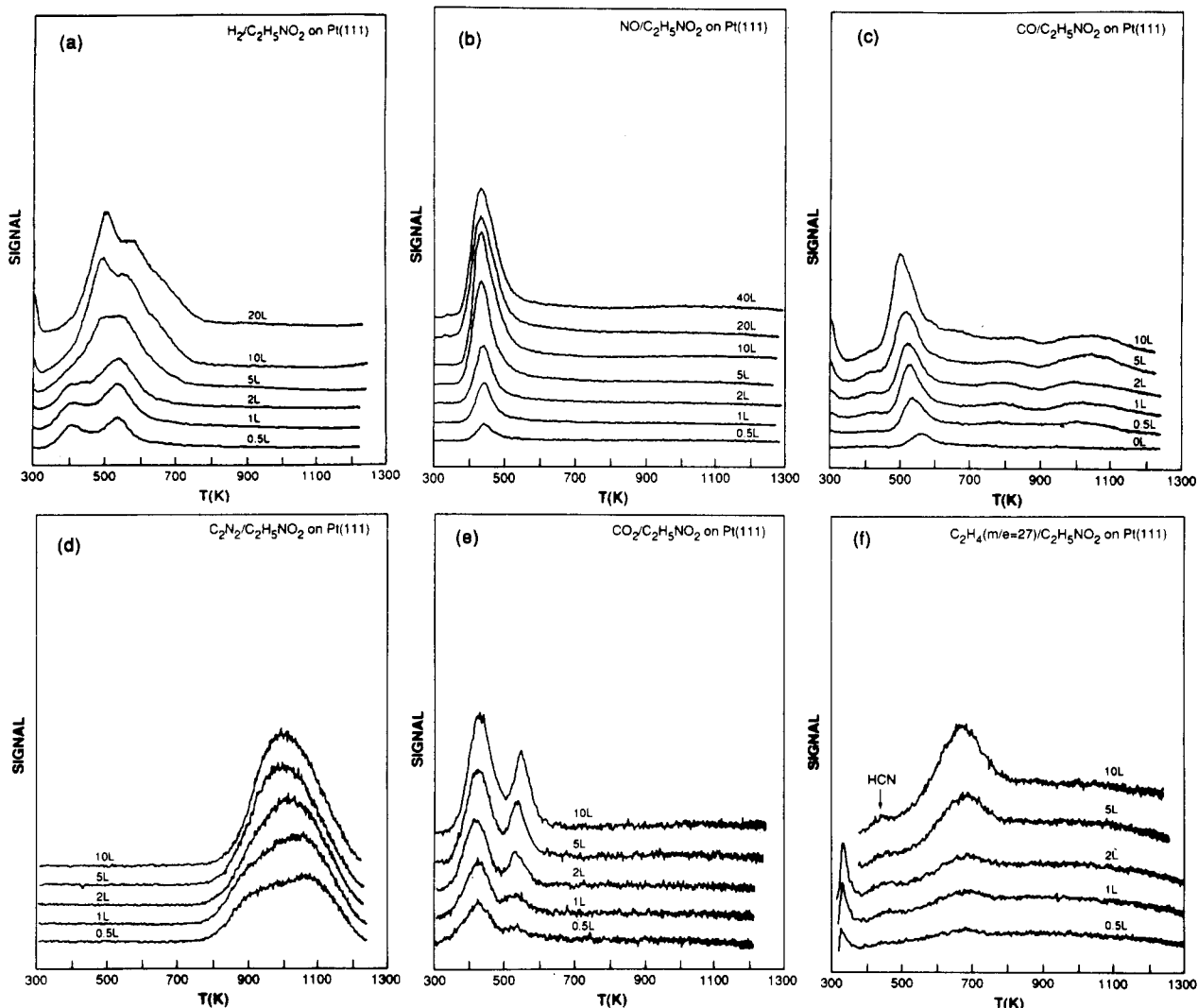


Figure 7. TPD spectra of (a) H_2 , (b) NO , (c) CO , (d) C_2N_2 , (e) CO_2 , and (f) C_2H_4 ($m/e = 26$) on Pt(111) following $C_2H_5NO_2$ exposures indicated at 300 K.

TABLE I: Yields^a of Desorption Products from Saturation Coverages of CH₃NO₂ and C₂H₅NO₂ on Rh(111) and Pt(111) [1] at 300 K

product	CH ₃ NO ₂		C ₂ H ₅ NO ₂	
	Pt(111)	Rh(111)	Pt(111)	Rh(111)
monolayer	1.72×10^{14}	2.68×10^{14}	1.24×10^{14}	1.85×10^{14}
C ₂ N ₂	0.75	<0.01	0.25	<0.01
HCN	0.02	0.02	<0.01	<0.01
N ₂	<0.01	1.30	<0.01	0.90
NO	0.20	0.06	0.74	0.05
C ₂ H ₄	<0.01	<0.01	0.03	1.39
H ₂	0.60	0.80	1.01	1.00
O ₂	<0.01	<0.01	<0.01	0.66
CO	0.22	1.40	0.41	0.65
CO ₂	0.03	0.48	0.05	0.29
CH ₄	0.02	0.11	<0.01	<0.01

^aAmounts were obtained from TPD peak areas with calibrations discussed in text. All yields are in molecules/cm².

C₂H₄ adsorption are also detected. This indicates that the C-N bond in C₂H₅NO₂ might be cleaved at low temperatures (<400 K).

NO desorbs as a single peak at ~430 K at low C₂H₅NO₂ coverages (Figure 7b). This peak shifts down in temperature with increasing C₂H₅NO₂ coverage to ~420 K at saturation (~20 langmuirs), which is comparable to the NO desorption temperature from CH₃NO₂¹ and NO¹¹ adsorbed on Pt(111) at low coverages. The peak therefore is desorption limited and possibly arises from decomposition of the adsorbed NO₂ species near room temperature.³²⁻³⁴

CO desorption spectra in Figure 7c indicate only one desorption peak at ~530 K at low coverages. This peak shifts downward with increasing C₂H₅NO₂ exposure to ~490 K at saturation (~20 langmuirs). This peak matches that observed for low CO coverage on Pt(111)¹⁰ and is therefore desorption limited. At higher coverages, at least three sharp peaks at ~570, 660, and 780 K and a broad peak between 920 and 1160 K are observed. The broad peak between 920 and 1160 K is attributed to cracking fragments of C₂N₂ (Figure 7d) in the mass spectrometer. This is also observed from the C₂N₂ desorption from Rh(111) in the companion C₂N₂ and CH₃NH₂ paper. The three sharp peaks at 570, 660, and 780 K follow the H₂ desorption peaks at 550, 640, and 710 K and are attributed to oxidation of the carbon residues from the dehydrogenation of the surface C_nH species.

Cyanogen desorbs as two peaks at 910 and 1080 K at 0.5 langmuir (Figure 7d). These two peaks match those observed from adsorption of CH₃NO₂ and C₂N₂ on Pt(111) at low coverages¹ and are therefore attributed to recombination of adsorbed CN species. The two peaks overlap strongly above 1 langmuir, becoming indistinguishable at higher coverages with an apparent peak temperature of 1000 K, and are saturated at a low C₂H₅NO₂ coverage below 5 langmuirs.

CO₂ desorbs as two peaks at 420 and 530 K at 0.5 langmuir (Figure 7e). Both peaks are clearly reaction limited since CO₂ does not chemisorb on Pt(111). The peak at 420 K does not shift with increasing C₂H₅NO₂ coverage while the 530 K peak shifts up to ~550 K at 10 langmuirs where both peaks saturate. The 420 K peak is attributed to oxidation of carbon residues which arise from cleavage of the C-C bond of the first few langmuirs exposure of C₂H₅NO₂ which is evident from the desorption and saturation of C₂N₂ at low coverages. The CO₂ peak at 550 K coincides with the H₂ desorption peak at 550 K and the CO desorption peak at 570 K. It is therefore attributed to oxidation of the surface carbon species which arises from the C_nH → C + 1/2 H₂ reaction. CO₂ desorption was complete by 600 K. Figure 7f shows a broad C₂H₄ desorption peak at ~680 K. Calibration

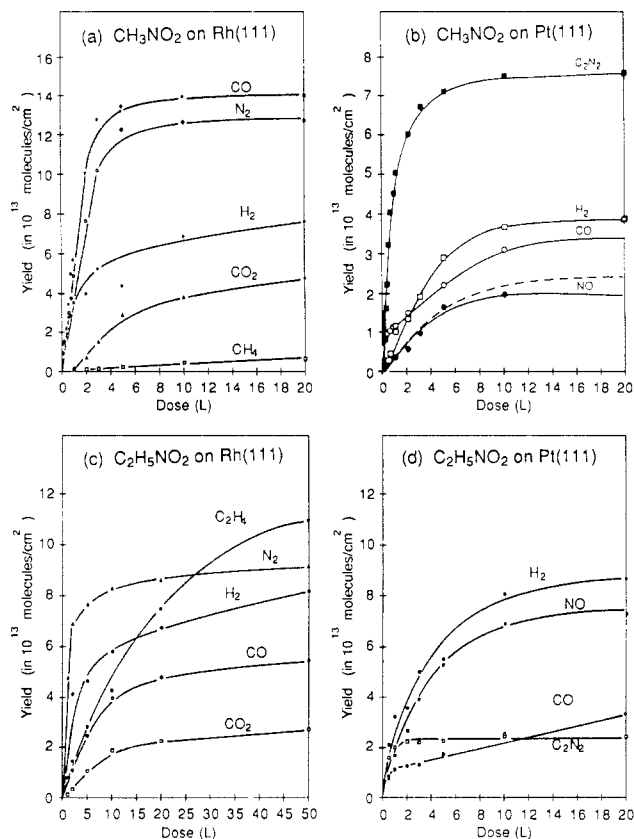


Figure 8. Yields of desorption products from adsorption of CH₃NO₂ on (a) Rh(111) and (b) Pt(111), and C₂H₅NO₂ on (c) Rh(111) and (d) Pt(111) as a function of exposure at 300 K. Amounts were obtained from TPD peak areas with calibrations discussed in text.

of the TPD peak area indicates that the peak is small and accounts for only ~1% of the total desorption products.

4. Adsorbate Coverages and Sticking Coefficients. Yields of desorption products from saturation coverages of CH₃NO₂ and C₂H₅NO₂ on Rh(111) at 300 K were calibrated against CO,⁴ NO,⁵ H₂,⁶ and O₂⁵ saturation densities on Rh(111), and those from C₂H₅NO₂ on Pt(111) at 300 K against C₂N₂,⁷ H₂,⁸ CO,^{9,10} and NO¹¹ saturation densities on Pt(111). These yields together with those of CH₃NO₂ on Pt(111)¹ are listed in Table I. We assume in the calculation that all C and N species desorb above 300 K so that C and N atom balances are possible, while H and O balances are obtainable only by differences because of desorption of H₂ and H₂O below 300 K. The saturation densities of CH₃NO₂ and C₂H₅NO₂ on Rh(111) and C₂H₅NO₂ on Pt(111) at 300 K (based on N atoms) are estimated to be 2.6×10^{14} , 1.9×10^{14} , and 1.2×10^{14} molecules/cm², respectively.

The carbon-nitrogen balance from Table I indicates that 25% of the carbon from CH₃NO₂ adsorption on Rh(111) and 59% from C₂H₅NO₂ on Pt(111) was left on the surface after thermal desorption to 1300 K, while C₂H₅NO₂ on Rh(111) and CH₃NO₂ on Pt(111)¹ do not leave any carbon residue. The carbon residue of CH₃NO₂ on Rh(111) and C₂H₅NO₂ on Pt(111) was also observed with AES and with changes in TPD spectra after a few high-exposure thermal desorption experiments.

Table I also indicates oxygen and hydrogen deficiencies compared to N atom in all systems. These deficiencies may arise from dehydrogenation and deoxygenation of adsorbates upon adsorption at 300 K followed by oxidation of the adsorbed H atoms to H₂O (the H₂ + O₂ → H₂O reaction is fast on Pt(111) at ~300 K³⁵) and desorption of H₂O at 300 K (the H₂O desorption temperature is ~180 K on Rh(111) and Pt(111)³⁶⁻³⁸).

(28) Baró, A. M.; Ibach, H. *J. Chem. Phys.* **1981**, *74*, 4194.

(29) Salmerón, M.; Somorjai, G. A. *J. Phys. Chem.* **1982**, *86*, 341.

(30) Greighton, J. R.; White, J. M. *Surf. Sci.* **1983**, *129*, 327.

(31) McCabe, R. W.; Schmidt, L. D. *Surf. Sci.* **1977**, *65*, 189.

(32) Segner, J.; Vielhaber, W.; Ertl, G. *Isr. J. Chem.* **1982**, *22*, 375.

(33) Dahlgren, D.; Hemminger, J. C. *Surf. Sci.* **1982**, *123*, L739.

(34) Bartram, M. E.; Windham, R. G.; Koel, B. E. *Surf. Sci.* **1987**, *184*,

(35) Zhdanov, V. P. *Surf. Sci.* **1986**, *169*, 1.

(36) Kiss, J.; Solymosi, F. *Surf. Sci.* **1986**, *177*, 191.

(37) Wagner, F. T.; Moylan, T. E.; Schmiege, S. J. *Surf. Sci.* **1988**, *195*, 403.

Figure 8 shows yields of desorption products from adsorption of CH_3NO_2 on (a) Rh(111) and (b) Pt(111) and $\text{C}_2\text{H}_5\text{NO}_2$ on (c) Rh(111) and (d) Pt(111) as a function of exposure at 300 K. Figure 8a indicates that only very small amounts of CO_2 and CH_4 were observed at 1 langmuir and that no CO_2 or CH_4 desorption was observed below 1 langmuir. All the desorption products from CH_3NO_2 adsorption saturate at ~ 40 langmuirs with no more than a few percent increase in peak areas at exposures up to 100 langmuirs. The initial sticking coefficient estimated from the slope of nitrogen curve gives $S_0 = 0.4$, a factor of 2 lower than the calculated value on Pt(111) (Figure 8b, and ref 1).

Among the desorption products from $\text{C}_2\text{H}_5\text{NO}_2$ adsorption on Rh(111) (Figure 8c), oxygen (data not shown) is the only product that saturates below 50 langmuirs; all other products continue to grow beyond 50 langmuirs and saturate between 100 and 200 langmuirs with 5–25% increase in peak areas compared with those at 50 langmuirs. Oxygen desorption from $\text{C}_2\text{H}_5\text{NO}_2$ saturates between 20 and 50 langmuirs with a yield of 6.6×10^{13} molecules/cm². Desorption amounts of CO_2 and C_2H_4 are very small at 1 langmuir and no desorption of these two products was observed below 1 langmuir. The initial sticking coefficient, S_0 , was estimated to be ~ 0.5 from the slope of nitrogen curve in Figure 8c.

All the desorption products from $\text{C}_2\text{H}_5\text{NO}_2$ exposure on Pt(111) at 300 K saturate below 40 langmuirs (Figure 8d). At low exposures (< 1 langmuir), C_2N_2 yield is higher than that of NO while NO yield is higher than that of C_2N_2 at high exposures. In fact, C_2N_2 saturates below 5 langmuirs while NO continues to grow until the peak saturates at ~ 20 langmuirs with a yield at saturation ~ 3 times that of C_2N_2 . This suggests that the C-N bond in $\text{C}_2\text{H}_5\text{NO}_2$ is not activated at low coverages but is cleaved at higher coverages. The initial sticking coefficient S_0 is estimated to be ~ 0.6 from the initial slope of the $\text{NO} + 2\text{C}_2\text{N}_2$ curve in Figure 8d.

Discussion

1. CH_3NO_2 on Rh(111). Figure 9a represents our interpretation of the steps in CH_3NO_2 decomposition on Rh(111). Shown in the figure are TPD peak temperatures for the major products and possible surface species. All CH_3NO_2 which adsorbs on Rh(111) either desorbs at 165 K (multilayer) or at 180 K (second monolayer) or reacts to form CO , N_2 , H_2 , CO_2 , and other minor products. Carbon residues were observed after the surface was annealed to 1250 K.

From thermal desorption data, it is evident that the first CH_3NO_2 monolayer decomposes completely below 400 K to leave CH_x because CO_2 desorbs as a reaction-limited peak with a peak temperature of 405 K, which is identical with that from $\text{CO} + \text{NO}$ and $\text{CO} + \text{O}_2$ adsorption on Rh(111).¹⁵ The scission of the C-N bond in CH_3NO_2 must precede that of both N-O bonds, since, if a surface H_xCN species ever existed, it would dehydrogenate completely by 480 K to CN, which is stable on Rh(111) up to 800 K as shown in the companion C_2N_2 and CH_3NH_2 paper. In other words, surface H_xCN or CN is never formed in the thermal desorption of CH_3NO_2 on Rh(111). This is in sharp contrast with CH_3NO_2 on Pt(111)¹ and CH_3NH_2 on Pt(111)² and Rh(111) where surface H_xCN and CN species were clearly indicated.

Since NO_2 decomposes readily to NO on Rh³⁹ and Pt(111),³²⁻³⁴ and NO dissociates rapidly on Rh(111) at temperatures above 275 K even at high NO coverages,¹⁵ the N-O bonds in CH_3NO_2 must break shortly after the cleavage of the C-N bond. This is indicated by the small NO desorption peak in Figure 1. In fact, more than 97% of the N atoms which adsorb on Rh(111) desorb as N_2 .

Following CO_2 desorption at 405 K, the major species remaining on the surface should be N and O atoms and CH_x species which dehydrogenate at 480, 550, and 630 K (forming reaction-limited H_2) to leave surface carbon residues. The CO and CO_2 peaks

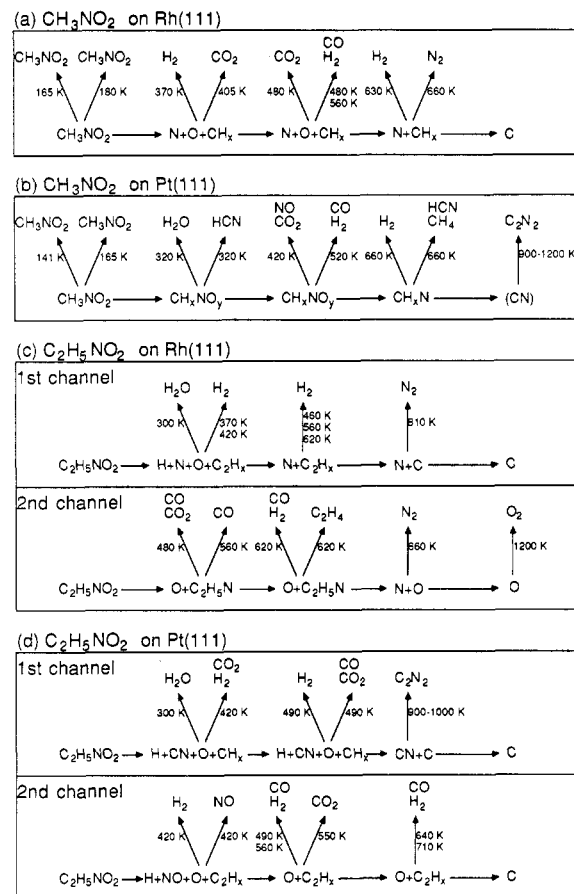


Figure 9. Reaction path of CH_3NO_2 on (a) Rh(111) and (b) Pt(111)¹ and $\text{C}_2\text{H}_5\text{NO}_2$ on (c) Rh(111) and (d) Pt(111).

at 480 K coincide with the H_2 desorption peak at the same temperature, which suggests that these peaks are from the same reaction: oxidation of the carbon residue arising from dehydrogenation of some CH_x species at 480 K.

Following the dehydrogenation of the CH_x species at 550 K, a significant amount of CO desorbs as a peak at 560 K, but no significant CO_2 desorption was observed at that temperature. This is quite different from CH_x dehydrogenation at 480 K, where comparable amounts of CO and CO_2 were produced. This suggests that, at 560 K, the oxidation reaction is limited by the amount of O atoms remaining on the surface. The absence of significant CO or CO_2 desorption peaks following the dehydrogenation of CH_x at 630 K indicates that surface O atoms are depleted at ~ 600 K. The only major species remaining on the surface above 600 K are CH_x and N atoms, which desorb as N_2 at 660 K. At 800 K, no more desorption occurs, and the only species on the surface is carbon residue.

Comparison of the CH_3NO_2 decomposition paths on Rh(111) and Pt(111) (Figure 9a,b)¹ suggests that the key to the striking difference in CH_3NO_2 thermal desorption products on the two metals is the stability of the C-N bond. On Pt(111), 85% of the C-N bonds remain stable up to 1000 K and then desorb as C_2N_2 , while all the C-N bonds on Rh(111) are completely cleaved below 400 K, leaving surface N and O atoms and CH_x species, which can only dehydrogenate to surface carbon residues.

Comparison of CH_3NO_2 and CH_3NH_2 decomposition on Rh(111) reveals some interesting differences in the stability of the C-N bonds on these two metals. The C-N bond in CH_3NH_2 is stable up to ~ 800 K where it decomposes to N_2 and surface carbon, while in CH_3NO_2 the bond is cleaved below 400 K. The presence of oxygen atoms in the CH_3NO_2 molecule therefore reduces the stability of the C-N bond significantly by weakening the C-N bond (the C-N bond energy is 87 kcal/mol in CH_3NH_2 and 62 kcal/mol in CH_3NO_2) and by altering the adsorption bonding of the molecules on the surface. The CH_3NH_2 molecule

(38) Fisher, G. B.; Gland, J. L. *Surf. Sci.* **1980**, *94*, 446.

(39) Papapolymerou, G. A.; Schmidt, L. D. *Langmuir* **1985**, *1*, 488.

should adsorb on Rh(111) through nitrogen lone pair electrons as on Ni and Cr surfaces^{40,41} while the CH_3NO_2 molecule can only bond to Rh either through oxygen or through the π bonds in the nitro group. It is probable that CH_3NO_2 bonds to the Rh surface through the π bonds in the nitro group, making the C–N bond parallel to the metal surface and bringing the carbon atom closer to the metal than in CH_3NH_2 . This would facilitate scission of the C–N bond in CH_3NO_2 to adsorbed CH_3 and NO_2 species which then decompose to adsorbed N, O, and CH_x .

The combination of the C–N bond weakening and adsorption bonding alteration has different effects on decomposition of CH_3NO_2 on Pt(111) and Rh(111). The effect is only modest on Pt(111): the stability of C–N bond is reduced from no C–N bond scission up to 1200 K in CH_3NH_2 ² to 15% C–N bond scission below 500 K in CH_3NO_2 .¹ On Rh(111), the effect is more pronounced: from 39% C–N bond scission at ~ 800 K in CH_3NH_2 to complete C–N bond scission below 400 K. However, both surfaces show the same trend toward the two adsorbates: the C–N bond in CH_3NH_2 is more stable than that in CH_3NO_2 .

2. $\text{C}_2\text{H}_5\text{NO}_2$ on Rh(111). From the absence of major desorption peaks of CO, CO_2 , C_2H_4 , and O_2 at low $\text{C}_2\text{H}_5\text{NO}_2$ exposures and their becoming the dominant products at saturation, it is evident that $\text{C}_2\text{H}_5\text{NO}_2$ decomposes on Rh(111) through at least two reaction channels with one dominating at low coverages and one at high coverages. Figure 9c illustrates our interpretation of the two reaction channels.

At low coverages, the $\text{C}_2\text{H}_5\text{NO}_2$ molecule adsorbs on Rh(111) readily, presumably through the π bonds in the nitro group, and decomposes completely to surface H, N, and O atoms and C_2H_x species (most likely ethylidyne, C_2H_3) which dehydrogenate at 420, 460, 560, and 620 K to leave surface carbon residues. From the reduction of the hydrogen desorption peak at 370 K and the absence of major CO and CO_2 desorption peaks following the dehydrogenation of C_2H_x , as in CH_3NO_2 on Rh(111), it is clear that surface oxygen is depleted below 400 K, where the first CO_2 desorption peak should emerge. This oxygen loss at low temperature should arise from the $2\text{H}_{\text{ad}} + \text{O}_{\text{ad}} \rightarrow \text{H}_2\text{O}$ reaction near 300 K. Therefore, the only major species on the Rh surface at 400 K should be C_2H_x and N. Above 400 K, N atoms form N_2 at 680–800 K,¹⁷ and C_2H_x forms C_2H_4 which desorbs at 750 K.

Since the adsorption of $\text{C}_2\text{H}_5\text{NO}_2$ through the π bonds in the nitro group has at least four atoms close to the surface, it should occupy more adsorption sites than by bonding through the oxygen atoms, which has only two O atoms on the surface. As a result, although $\text{C}_2\text{H}_5\text{NO}_2$ can bond to the surface through π bonds at low coverages, it can only adsorb on the surface through the oxygen atoms above certain coverages. The molecules adsorbed at high coverages then follow the second channel which leads to different desorption products.

Because of the bonding of the O atoms to the Rh surface, the N–O bonds in $\text{C}_2\text{H}_5\text{NO}_2$ should be weakened from a bond order of 1.5 to 1, or from a N–O bond energy close to that in NO_2 (73 kcal/mol) to that in $\text{CH}_3\text{N–OH}$ (50 kcal/mol). The weakened N–O bonds then cleave readily below 350 K as evidenced by the CO_2 desorption that starts at the same temperature to leave adsorbed O atoms and $\text{C}_2\text{H}_5\text{N}$ species which decompose to C_2H_4 , H_2 , and surface N atoms between 360 and 750 K.

The desorption of C_2H_4 exhibits certain characteristics that indicate the processes that produce it. C_2H_4 desorption should arise solely from decomposition of the surface $\text{C}_2\text{H}_5\text{N}$ species since its desorption spectra reveal only one major peak and hydrogenation of adsorbed ethylidyne species (from the first channel) to C_2H_4 has been shown to be unlikely.^{19,20} Judging from the desorption peak at 620 K, which is common to C_2H_4 and H_2 , the scission of C–H and C–N bond in $\text{C}_2\text{H}_5\text{N}$ probably occurs simultaneously, making the process a pseudo-one-step process unlike the decomposition of the C_2H_3 species which occurs in several steps. From this, we should expect C_2H_4 desorption to be a single

peak. However, the C_2H_4 desorbs as a broad peak between 360 and 750 K. This suggests that decomposition of the $\text{C}_2\text{H}_5\text{N}$ species to C_2H_4 is limited by the availability of adjacent vacant sites on an obviously crowded surface since the process requires several adjacent sites for adsorption of fragments.

The two reaction channels are therefore not independent. Above 400 K, the C_2H_x species (from the first channel) dehydrogenates in several peaks to H_2 and surface carbon, which is oxidized immediately by oxygen atoms (from the second channel) to CO and CO_2 . This process then produces some vacant sites to allow decomposition of the $\text{C}_2\text{H}_5\text{N}$ species (from the second channel) to C_2H_4 , H_2 , and adsorbed N atoms. The two reaction channels couple strongly until the decomposition and oxidation of the C_2H_x species (indicated by H_2 and CO desorption) and the decomposition of the $\text{C}_2\text{H}_5\text{N}$ species (C_2H_4 and H_2 desorption) cease simultaneously at 750 K. At 750 K, the only species remaining on the surface should be O and N atoms which desorb as N_2 by 880 K. The adsorbed O atoms desorb as O_2 at 1200 K.

3. $\text{C}_2\text{H}_5\text{NO}_2$ on Pt(111). From the saturation of C_2N_2 at low $\text{C}_2\text{H}_5\text{NO}_2$ exposure and the saturation of NO and H_2 at high exposure, it is evident that the decomposition of $\text{C}_2\text{H}_5\text{NO}_2$ on Pt(111) must also follow at least two reaction channels with one dominating at low $\text{C}_2\text{H}_5\text{NO}_2$ exposures and another one dominating at saturation. Figure 9d represents the two reaction channels we propose with the first channel producing C_2N_2 as the major product at low coverages and the second producing NO as the major product at saturation, just as on Rh(111). However, the presence of a significant amount of NO desorption at low coverages (Figure 7b) indicates that the transition between the two reaction channels is not as distinct as on Rh(111), where no significant desorption of O_2 and C_2H_4 from the second channel was observed below 5 langmuirs and no carbon residue (a major product from the first channel) was left on the surface at saturation. On Pt(111), it is estimated that the first channel dominates over the second channel by 2 to 1 at low coverages and the second over the first by 3 to 1 at saturation.

At low coverages, we expect the $\text{C}_2\text{H}_5\text{NO}_2$ molecules to adsorb on Pt(111) through the π bonds in the nitro group as on Rh(111) and decompose to surface H, O, CH_x , and CN species below 400 K as evidenced by the CO_2 desorption peak at 420 K. The C–N bond in $\text{C}_2\text{H}_5\text{NO}_2$ in this case is not cleaved as on Rh(111) due to its high stability on Pt(111) as indicated by the thermal desorption of C_2N_2 , CH_3NH_2 ² and CH_3NO_2 .¹

Above 340 K, the CH_x species begins to dehydrogenate in at least two peaks at 420 and 530 K to surface carbon, which is readily oxidized to CO and CO_2 as evidenced by the H_2 and CO_2 desorption peaks near 420 and 530 K and CO desorption at ~ 540 K. No CO desorption at 420 K was observed since it is desorption limited. At 650 K, the desorption of all H and O containing molecules is complete and the only species remaining on the surface should be CN and a small amount of carbon residue predicted from the small carbon deficiency in the gaseous product at low $\text{C}_2\text{H}_5\text{NO}_2$ exposures (Figure 8d). The CN species then recombine and desorb as C_2N_2 between 780 and 1300 K.

The second reaction channel (Figure 9d) should begin with $\text{C}_2\text{H}_5\text{NO}_2$ molecules adsorbed on the Pt surface through the oxygen atoms since this should dominate at high $\text{C}_2\text{H}_5\text{NO}_2$ coverages. However, the fact that significant amounts of NO were produced even at low coverages suggests that π bonding is not favored over bonding through O atoms (the second channel) on Pt(111) as on Rh(111). This may arise from a stronger Pt–O bond (180 ± 4 kcal/mol) than the Rh–O bond (90 ± 15 kcal/mol), which makes the bonding through π bonds favored energetically over that through O atoms to a lesser extent on Pt(111) than on Rh(111).

Following adsorption of $\text{C}_2\text{H}_5\text{NO}_2$ through the O atoms (the second channel), the molecules readily decompose to adsorbed H, O, NO, and C_2H_x species below 370 K as evidenced by the NO desorption which starts at the same temperature. It is not understood why the C–N bond breaks on Pt(111) but not on Rh(111) through the same bonding (O atoms). Since NO desorbs as a desorption-limited peak at 420 K,¹¹ it should be produced

(40) Baca, A. G.; Schulz, M. A.; Shirley, D. A. *J. Chem. Phys.* **1985**, *83*, 6001.

(41) Schoofs, G. R.; Benziger, J. B. *J. Phys. Chem.* **1988**, *92*, 741.

near 300 K. Above 400 K, C_2H_x begins to dehydrogenate in at least four peaks at 490, 560, 640, and 710 K to surface carbon as in C_2H_4 adsorption on Pt(111). Some of the surface carbon is oxidized readily to CO (desorption at 490, 570, 660, and 780 K) and CO_2 (550 K). AES reveals that some carbon residues are left on the surface after TPD to 1300 K.

Summary

CH_3NO_2 decomposes completely on Rh(111) below 400 K by scission of N-O bonds to form CH_xN and CH_x species which dehydrogenate to surface carbon completely by ~ 750 K to produce CO, N_2 , H_2 , and CO_2 . This is in sharp contrast with Pt(111) on which C_2N_2 and H_2 are the major products.

Decomposition of $C_2H_5NO_2$ on Rh(111) is quite different than CH_3NO_2 in that considerable C_2H_4 is formed. Decomposition is described by two reaction channels which begin with different adsorption bonds and yield different products. Through the first channel, which dominates at low coverages, $C_2H_5NO_2$ probably bonds to the surface through the π bonds in the nitro group and decomposes readily to H, N, and O atoms and C_2H_x species which dehydrogenate between 420 and 620 K to leave surface carbon. Through the second channel, which dominates at high coverages,

$C_2H_5NO_2$ remains partially intact, perhaps as a C_2H_5N species which decomposes to C_2H_4 , H_2 , and N_2 between 360 and 750 K. At saturation, $\sim 70\%$ of the C desorbs as C_2H_4 with the remainder desorbing as CO and CO_2 .

$C_2H_5NO_2$ decomposition on Pt(111) is also described by two competing reaction channels which yield different major products. At low coverages (first channel), $C_2H_5NO_2$ adsorbs through the π bonds as on the Rh surface and decomposes to H, O, CH_x , and CN species which desorb as C_2N_2 between 780 and 1300 K. At higher coverages the second channel opens and $C_2H_5NO_2$ bonds to the surface through the O atoms and decomposes below 370 K to H, O, C_2H_x , and NO, which desorbs as a desorption-limited peak at 420 K. The C_2H_x species then dehydrogenates in several peaks between 490 and 710 K to surface carbon. At saturation, $\sim 60\%$ of the N atoms desorb as NO and the rest as C_2N_2 .

Acknowledgment. This research was partially supported by NSF under Grant No. DMR82126729.

Registry No. H_2 , 1333-74-0; N_2 , 7727-37-9; CO_2 , 124-38-9; O_2 , 7782-44-7; CO, 630-08-0; C_2H_4 , 74-85-1; NO, 10102-43-9; C_2N_2 , 460-19-5; nitromethane, 75-52-5; nitroethane, 79-24-3; platinum, 7440-06-4; rhodium, 7440-16-6.

Activation of Aromatics on the Polar Surfaces of Zinc Oxide

J. M. Vohs[†] and M. A. Barteau*

Center for Catalytic Science and Technology, Department of Chemical Engineering, University of Delaware, Newark, Delaware 19716 (Received: April 4, 1989; In Final Form: June 15, 1989)

The reactions of the aromatic oxygenates benzoic acid, benzaldehyde, benzyl alcohol, and phenol exhibit both strong similarities and strong differences as compared with their aliphatic analogues on the two polar surfaces of zinc oxide. The greatest similarities between aromatic and aliphatic compounds were observed on the (0001)-Zn polar surface. Benzoic acid and benzaldehyde reacted on the (0001)-Zn surface to form surface benzoate species. Decomposition of surface benzoates resulted in the production of small amounts of benzene and the deposition of a carbonaceous residue on the surface. This carbonaceous layer was oxidized by lattice oxygen to carbon oxides at temperatures greater than 750 K. Benzyl alcohol and phenol reacted on the (0001)-Zn surface to form the corresponding surface alkoxide species. These alkoxides were unusually stable and, unlike their aliphatic analogues, did not react with lattice oxygen to form surface carboxylate species; rather they decomposed directly at temperatures greater than 800 K. In sharp contrast to aliphatic alcohols, aldehydes, and carboxylic acids, toward which the (0001)-O polar surface is unreactive, the aromatic compounds reacted on the (0001)-O polar surface. During TPD experiments benzoic acid, benzaldehyde, and phenol decomposed on the (0001)-O polar surface to produce CO, CO_2 , H_2 , and H_2O , which desorbed at temperatures greater than 700 K. The XPS and UPS spectra of the adsorbed species demonstrated that the aromatic compounds did not adsorb dissociatively on the (0001)-O polar surface but rather were stabilized by direct interaction of the phenyl ring with the surface. These results further demonstrate the effects of surface crystallographic structure in determining the activity and reaction pathways on metal oxide surfaces. They demonstrate also the ability of different surface structures to activate different organic functional groups.

Introduction

In many industrial catalytic processes, the reactant and product streams contain a variety of aromatic compounds; this is particularly true in petroleum refining where light aromatics are used to increase the octane number of gasoline. These streams may also be used as feedstocks for chemical production. For example, the partial oxidation of aromatic compounds such as toluene, *o*-xylene, and naphthalene over metal oxide catalysts has been practiced industrially to produce aromatic aldehydes, acids, and anhydrides.^{1,2} A number of metal oxides, including V_2O_5 , MoO_3 , and ZnO, are known to be active for the oxidation of aromatic compounds,¹⁻⁶ although the most commonly used industrial catalysts for the selective oxidation of aromatics consist of V_2O_5 or mixtures of V_2O_5 and other metal oxides. A knowledge of the interaction of aromatic compounds with metal oxide surfaces is

important to the understanding of these catalytic reactions.

In addition to catalytic processes, the interaction of aromatic compounds with metal oxide surfaces is important in several other fields. Aromatics are used as binders and adhesives in a wide variety of applications in which metal oxides are also used. For example, polymeric resins containing phenolic and other oxygenated aromatic moieties are used in polymer/ceramic fiber composite materials.^{7,8} Paints colored with metal oxide pigments

(1) Gates, B. C.; Katzer, J. R.; Schuit, C. G. A. *Chemistry of Catalytic Processes*; McGraw-Hill: New York, 1979.

(2) Satterfield, C. N. *Heterogeneous Catalysis in Practice*; McGraw-Hill: New York, 1980.

(3) Andersson, S. L. T. *J. Catal.* **1986**, *98*, 138.

(4) Chang, C. C.; Kokes, R. J. *J. Catal.* **1975**, *38*, 491.

(5) Sachtler, W. M. H. *Catal. Rev.* **1970**, *4*, 27.

(6) Margolis, L. Ya. *Catal. Rev.* **1974**, *8*, 241.

(7) Sheldon, R. P. *Composite Polymeric Materials*; Applied Science Publishers: London, 1982.

[†] Present address: Department of Chemical Engineering, University of Pennsylvania, Philadelphia, PA 19104.